

New Multi-messenger Probe of Dark Matter-Nucleon Interactions from Ultra-high Energy Cosmic Ray Acceleration

Stephan A. Meighen-Berger ^{1,2,3,*}, P. S. Bhupal Dev ^{4,†} and Matheus Hostert ^{3,‡}

¹*School of Physics, The University of Melbourne, Victoria 3010, Australia* 

²*Center for Cosmology and AstroParticle Physics (CCAPP),
Ohio State University, Columbus, OH 43210, USA* 

³*Department of Physics and Astronomy, University of Iowa, Iowa City, IA 52242, USA* 

⁴*Department of Physics and McDonnell Center for the Space Sciences,
Washington University, St. Louis, MO 63130, USA* 

It has been suggested that the density of dark matter (DM) halo can be highly enhanced around supermassive black holes at the centers of massive galaxies. If real, these DM *spikes* would offer new opportunities to probe the properties of DM. In this work, we point out that DM spikes can significantly impact the composition and survivability of ultra-high-energy cosmic rays accelerated near supermassive black holes. A large DM-nucleon cross section would fragment heavy nuclei into lighter elements and prevent them from attaining the energies observed at Earth. While the origin of cosmic rays remains a mystery, we show that if the highest-energy cosmic rays on Earth come from sources like NGC1068, then cross sections of size $\sigma_{\chi p} \leq 3 \times 10^{-34} \left(\frac{m_\chi}{\text{GeV}}\right) \text{cm}^2$ would be excluded by cosmic ray data. These bounds can be competitive with other existing probes in the DM mass region $m_\chi \in [5 \text{ MeV}, 50 \text{ MeV}]$. While the uncertainties on the acceleration mechanism of cosmic rays prevent us from setting robust limits, our study highlights an important connection between DM spikes and cosmic ray physics that is complementary to existing cosmological and direct detection constraints.

I. INTRODUCTION

Supermassive black holes (SMBH), believed to exist at the centers of almost all massive galaxies, provide extreme and naturally-occurring laboratories with which to probe the microphysics of cosmic rays (CRs), neutrinos, and dark matter (DM). These objects, with masses ranging from millions to billions of solar masses, create some of the most energetic environments in the Universe, where particles can be accelerated to ultra-high energies through various mechanisms including magnetic reconnection, shock acceleration, and interactions with accretion disk turbulence [1–8]. The recent discovery of NGC 1068 [9] as a high-energy neutrino source and its lack of corresponding TeV gamma-ray signal have shown that the close vicinity of the central SMBH is the most likely source of high-energy neutrino production [10]. The suppression of gamma rays, combined with the fact that this is the first steady source of neutrino observed, suggests that the emission region is deeply embedded within dense material that effectively absorbs high-energy electromagnetic radiation while allowing neutrinos to escape. This, in turn, implies that CRs are accelerated near the central SMBH, within a few to hundreds of Schwarzschild radii from the event horizon. These small distances would imply that the CR acceleration is taking place in an environment with a potentially large ambient DM density, assuming a cuspy profile.

Gamma-ray observations from other galaxies (e.g., NGC 4486) have also demonstrated that high-energy emission can originate from regions very close to the event horizon, supporting the plausibility of particle acceleration at these scales [18–23]. Such obscured,

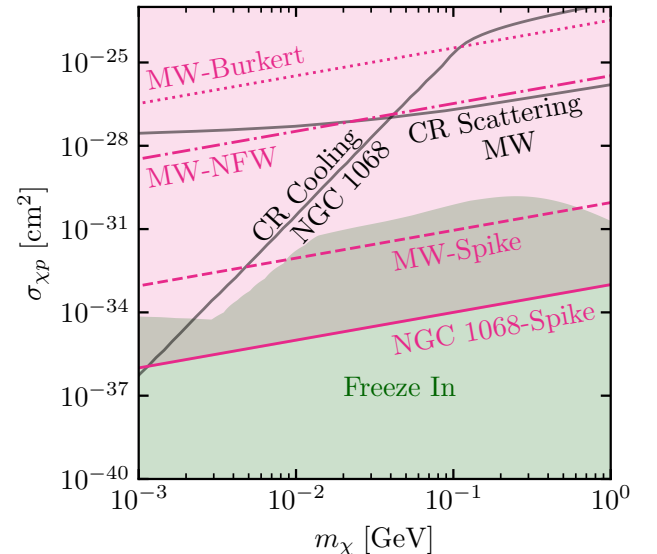


FIG. 1. The approximate bounds set here (pink region) using a spiked DM-density profile [11] in an NGC 1068-type galaxy compared to other proposed bounds using CRs (black lines). Specifically, we are showing scattering [12], and cooling [13] bounds. We also show DM-proton cross section values that can produce the correct relic abundance via freeze-in (green region) [14, 15]. Our potential bounds using a Burkert [16], NFW [17], and spiked-density profiles for Milky-Way-like galaxies are shown as dotted, dashed-dotted, and dashed lines, respectively.

Compton-thick sources have long been theorized [24–27], but their existence is only now being confirmed with the

advent of multi-messenger astronomy [28–30]. For instance, these obscured Active Galactic Nuclei (AGNs) have been used to explain the X-ray background (XRB) measurements [31], specifically the peak between 20–30 keV [32–35]. Interestingly, non-jetted AGNs have also been used to explain the XRB [36] and astrophysical neutrino background [37]. Similar arguments have also been recently applied to NGC 7469 [38].

While cuspy profiles are often used to describe DM halos, the presence of a SMBH can further enhance the DM density in its vicinity. It has been suggested that the DM density profile could form a ‘spike’ as we go closer to the SMBH due to adiabatic growth of the black hole [11]. In other words, as the central black hole forms and grows, its gravity pulls in ambient DM, compressing it into a much steeper density profile, referred to as a “spike”. The origin of a spiked profile can be theoretically motivated simply from angular momentum conservation. With more mass accreting onto the SMBH, the minimum of the effective gravitational potential shifts towards the center, thus giving rise to a spike profile.

Qualitatively, the spike formation can be understood as follows: Starting from an initial DM density profile $\rho(r) \propto r^{-\gamma}$ with γ an initial density slope (typically $0.5 \lesssim \gamma \lesssim 1.5$ [39–43]), the adiabatic growth of the black hole causes the orbits of DM particles to contract towards the center. This process, which conserves adiabatic invariants, results in a new power-law density profile within the spike, $\rho_{\text{sp}}^{\gamma_{\text{sp}}}(r) \propto r^{-\gamma_{\text{sp}}}$. The relationship between the initial slope γ and the spiked slope γ_{sp} is given by $\gamma_{\text{sp}} = \frac{9-\gamma}{4-\gamma}$ [11, 44]. For typical halo models where γ ranges from 0 to 2, this transformation yields very steep inner profiles, with γ_{sp} values between 2.25 and 2.5. The spike is theorized to extend from a minimum radius, influenced by annihilation or capture effects, out to a characteristic radius $R_{\text{sp}} \sim 1$ pc. These results were then improved by using a fully relativistic treatment [45].

The potential existence of these spikes has been leveraged in numerous analyses to enhance expected sensitivities for DM searches, including studies by FGST and PAMELA [46], various gamma-ray observations [47, 48], and stellar observations [49–51]. Furthermore, the spike has been utilized to set bounds on DM interactions through its capture and annihilation within stars [52] and to predict the existence of dark stars [53]. More recently [54] used the spike to explain the neutrino signal from NGC1068 via DM annihilation. Additionally, [55–58] have used spike profiles to constraint neutrino-DM interactions from IceCube and future galactic supernova neutrino observations. Collectively, these studies highlight the broad phenomenological relevance of spiked profiles. Note, however, that the existence of the spike is not yet established observationally and is still under debate [49, 59, 60]. See Appendix A for a review of possible mechanisms that could weaken or destroy such spikes.

In this paper, we discuss how the existence of a spiked DM halo impacts CR acceleration to ultra-high energies. These ultra-high energy CRs (UHECRs) are expected

predominantly to consist of heavier elements, including iron [61–71]. A single scattering event between such energetic CRs and a DM particle during the acceleration process would cause the heavy (iron) nucleus to shatter. If such fragmentation occurs, CRs would be unable to reach the observed ultra-high energies, particularly near the Greisen-Zatsepin-Kuzmin (GZK) cutoff [72, 73]. In fact, the observation of several super-GZK events [74–76] strongly suggest that (i) these UHECRs are most likely heavy nuclei (with higher GZK cutoff) rather than protons, and (ii) fragmentation of these heavy nuclei is unlikely to happen at the source.

Here we ask the question: *Can high-energy CRs be accelerated within the DM spike to the ultra-high energies necessary to explain current observations by CR experiments [64, 77]?* We split this question into three parts:

1. Can CRs be accelerated to the required energies within an AGN?
2. Can CRs be accelerated within their trapped region?
3. Can the CRs escape their host galaxy?

Given the observation of UHECRs on Earth, we can set bounds on the DM-nucleon cross section by requiring that the interaction length of CR-DM interactions is at least larger than the acceleration region. Figure 1 shows the approximate results we predict compared to other CR bounds. Not shown are bounds due to changes in the expected metallicity [78] measured by CR experiments such as AMS [79]. There, it is assumed the DM-nucleon cross section behaves as the proton-nucleon cross section, scaled by a phenomenological factor b_{χ} , $\sigma_{\chi-N} = b_{\chi}\sigma_{p-N}$. For instance, in some scenarios, the DM-nucleon cross section scales as $\sigma_{\chi-N} \sim A^{2/3} \ln^2(s)$, where A is the nucleon count, and \sqrt{s} the center of mass energy [80–85]. With such a scaling, we would have to *improve* our bounds by $\mathcal{O}(100)$ to compare with [78] and $\mathcal{O}(1000)$ to compare with direct detection experiments. Since we wish to remain agnostic to the underlying model, we assume $\sigma_{\chi-N}$ is constant with the momentum transfer.

Note, that the method presented here is similar to [12, 78]. The main difference is that the authors focused on changes in the energy spectrum (at lower energies) due to multiple scattering. In contrast, here we focus on single-scatter events at higher energies.

This article is structured as follows. In Section II, we briefly discuss the DM-density profiles used in this work and in Section III we discuss general CR-DM interactions. Then, in Section IV, we derive bounds using EeV CR iron nuclei by requiring that it does not fragment during acceleration to these energies. We present our conclusions in Section V.

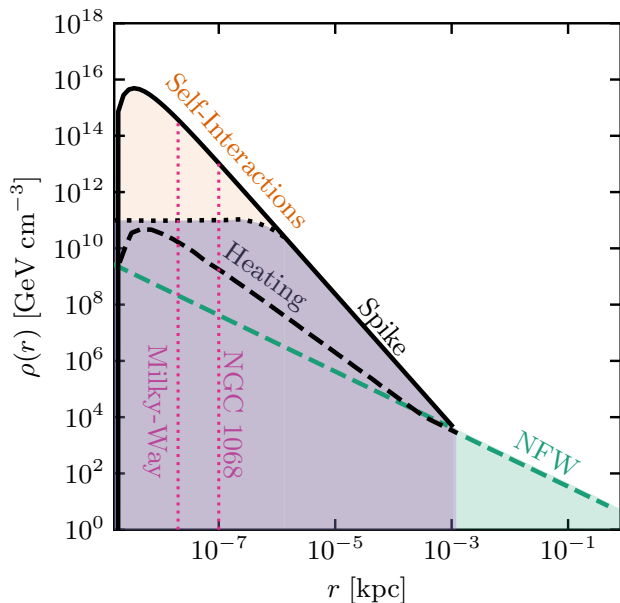


FIG. 2. The DM density as predicted by [11] combined with the NFW [17] profile starting at $r = 4R_S = 1.6 \times 10^{-9}$ kpc. The orange region shows where DM self-interactions (e.g., annihilation) could reduce the expected density. The black dashed line denotes the expected DM density when accounting for significant stellar heating [48], and the dotted black line indicates the plateau induced by an annihilation of $\langle\sigma v\rangle \sim 10^{-25}$ cm³/s. The pink vertical lines indicate the conservative acceleration regions of CRs for a Milky-Way-like or NGC1068-like galaxy, respectively, based on multi-messenger observations.

II. DM DENSITIES

To model the DM density profile near the SMBH, we follow the formalism of [11]. We adopt a generalized NFW profile [17] for the ambient dark-matter halo outside of the spike region, with an initial slope parameter γ set to 1 and $\rho_0 = 0.4$ GeV/cm³, the local ($r_0 = 8.5$ kpc) dark matter density. In the simplest scenario, where the central SMBH grows adiabatically, via the slow in-fall of gas, the DM density can be written as

$$\rho_{\text{sp}}^{\gamma_{\text{sp}}}(r) \approx \rho_0 \left(\frac{R_{\text{sp}}}{r_0}\right)^{-\gamma} \left(1 - 4\frac{R_S}{r}\right)^3 \left(\frac{R_{\text{sp}}}{r}\right)^{-\gamma_{\text{sp}}}. \quad (1)$$

Here $R_S = 2GM_{\text{BH}}$ is the Schwarzschild radius of the black hole, $R_{\text{sp}} = \alpha_\gamma r_0 (M_{\text{BH}}/(\rho_0 r^3))^{1/(3-\gamma)}$ the size of the spike, and α_γ the normalization to match the density outside of the spike (here for $\gamma = 1 \rightarrow \alpha_\gamma = 0.12, \gamma_{\text{sp}} = 7/3$). Thus, the full density profile is

$$\rho_\chi(r) = \begin{cases} 0 & r < 4R_S \\ \rho_{\text{sp}}^{7/3}(r) & 4R_S \leq r \leq R_{\text{sp}} \\ \rho_{\text{NFW}}(r) & r \geq R_{\text{sp}} \end{cases}, \quad (2)$$

where $\rho_{\text{sp}}^{7/2}$ is the DM density with the spike parameter $\gamma_{\text{sp}} = 7/2$. There are multiple ways the above adiabatic accumulation of DM could be perturbed. For example, first, stars orbiting the central black hole can soften the spike via gravitational heating of the DM, and, if significant, can change the expected DM profile. This is reflected by the change in expected γ_{sp} . For the Milky-Way with the profile given above $\gamma_{\text{sp}} = 7/3 \rightarrow \gamma_{\text{sp}} = 3/2$ [48, 86, 87]. Secondly, if DM self-interacts, e.g. via annihilation, then the maximum of the spike would be reduced to ρ_c [11, 48, 54]. Here $\rho_c = m_\chi / (\langle\sigma v\rangle t_{\text{BH}})$ with m_χ the DM mass, $\langle\sigma v\rangle$ the thermally averaged annihilation cross-section, and t_{BH} the age of the SMBH. Combined, the resulting DM distribution (for the Milky-Way) would be

$$\rho_\chi^{\text{MW}}(r) = \begin{cases} 0 & r < 4R_S^{\text{MW}} \\ \frac{\rho_{\text{sp}}^{3/2}(r)\rho_c}{\rho_{\text{sp}}^{3/2}(r) + \rho_c} & 4R_S^{\text{MW}} \leq r \leq R_{\text{sp}}^{\text{MW}} \\ \frac{\rho_{\text{NFW}}(r)\rho_c}{\rho_{\text{NFW}}(r) + \rho_c} & r \geq R_{\text{sp}}^{\text{MW}} \end{cases}, \quad (3)$$

where $\rho_{\text{sp}}^{3/2}$ stands for the DM density in the spike with $\gamma_{\text{sp}} = 3/2$. Note, while in the above equations we set the lower spike bound to be $4R_S$, the lower bound could be as small as $2R_S$ [45, 56, 88].

Figure 2 shows the DM density profiles for the MW used in this work. We set $M_{\text{BH}} = 4 \times 10^6 M_\odot$, and $\gamma = 1$. Above one pc, the profile follows a standard NFW profile (green dashed), whereas below one pc, the spike takes over (solid black). The dotted line denotes the effects of self-annihilation when setting $\langle\sigma v\rangle = 10^{-25}$ cm³/s, while the black dashed line denotes the density profile when including stellar heating.

In the following we discuss CR acceleration within Milky-Way-like galaxies ($M_{\text{BH}} \sim 4 \times 10^6 M_\odot$ [89]), and NGC 1068-like galaxies ($M_{\text{BH}} \sim 8 \times 10^6 M_\odot$ [90]). This puts them at the low end of expected masses for SMBHs in AGNs, where we expected ranges from $10^6 M_\odot - 10^{10} M_\odot$ [91, 92]. Since the spike density scales with the mass of the SMBH as $\sim M^{0.7}$, using low masses, as we do here, should be considered a conservative approach.

III. DM COSMIC RAY INTERACTIONS

There are two relevant quantities needed for the discussion here. One is the momentum transfer during a CR and DM interaction event. The maximal momentum transfer can be written as [12, 93–95]

$$T_{\text{max}} = \frac{T_{\text{CR}}^2 + 2m_{\text{CR}}T_{\text{CR}}}{T_{\text{CR}} + (m_{\text{CR}} + m_\chi)^2/(2m_\chi)}. \quad (4)$$

Here we consider the energy transfer in the nucleus's rest frame, with $Q^2 = -t$, where t is the Mandelstam variable. Setting $Q^2 = -(p_\chi - p'_\chi)^2 > 0$, we get

$Q^2 = -2m_\chi^2 + 2m_\chi E'_\chi = 2m_\chi T'_\chi < 2m_\chi T_{\max}$. We now make the conservative requirement that $\sqrt{Q^2} \gtrsim 1$ GeV for iron to shatter, far above the binding energy of iron, $\epsilon_b \sim 9$ MeV, to ensure a thorough fragmentation. Therefore, requiring $m_\chi > 1 \text{ GeV}^2/2T_{\max} \simeq 1 \text{ GeV}^2/2T_{\text{CR}}$ implies that for 50 EeV, we require $m_\chi \gtrsim 0.01$ eV. For a more detailed discussion on momentum transfers and cross sections, see [96, 97].

We also define the interaction length, $\lambda_{\chi,\text{CR}}$ as

$$\lambda_{\chi,\text{CR}} = \frac{1}{n_\chi \sigma_{\chi\text{CR}}}, \quad (5)$$

where n_χ is the number density of DM and $\sigma_{\chi\text{CR}}$ the DM-Nucleus cross section.

Note that at the energies discussed here, we are beyond the regime of elastic scattering. For instance, for the scattering of a $T_{\text{iron}} = 100$ TeV iron CR on a $m_\chi = 0.1$ MeV DM target, the average momentum transfer is $\langle \Delta T \rangle \sim 4.5$ GeV, demonstrating that we are safely within the regime of deep inelastic scattering.

IV. IRON NUCLEI FRAGMENTATION

Here we focus on the possibility of accelerating iron to ultra-high energies near the SMBH and/or the inner jet, assuming a background dark-matter distribution with couplings to protons. See [98, 99] for reviews of possible models. Specifically, we ask the question: *Would a coupling to DM shatter the iron nuclei before it can accelerate to observed ultra-high energies?*

A. Accelerating within an AGN

Assuming UHECR near the GZK cut-off ($E_{\text{CR}} \sim 50$ EeV) are all accelerated within AGNs, we can set a basic requirement on the interaction length for CR-DM interactions, $\lambda_{\text{CR},\chi}$. The interaction length $\lambda_{\text{CR},\chi}$ needs to be *larger* than the acceleration distance l_{acc} of the CR. Otherwise, the CR (at these extreme energies assumed to be iron) would shatter and could not be accelerated to the necessary energies. Conservatively, we can set l_{acc} to the size of the AGN. Current observations set the size of AGNs to be $\lesssim 10^{-3}$ pc [100, 101]. Note here we define the size of the AGN to be the size of the accretion disk of the central SMBH.

Thus, assuming CR are accelerated within the accretion disk of the SMBH, we can set a conservative bound by setting $\lambda_{\chi,\text{CR}} \geq 10^{-3}$ pc. Using the previously defined DM-density profiles (at $r = 10^{-3}$ pc), we can then set a generic bound on $\sigma_{\chi,\text{CR}}$

$$\sigma_{\chi,\text{CR}} \leq \begin{cases} 1.2 \times 10^{-24} \left(\frac{m_\chi}{\text{GeV}}\right) \text{ cm}^2 & \text{for NFW} \\ 1.3 \times 10^{-28} \left(\frac{m_\chi}{\text{GeV}}\right) \text{ cm}^2 & \text{for Spike} \end{cases} \quad (6)$$

While these bounds are negligible for DM masses above 1 keV compared to current constraints [102, 103], for lower

masses they begin to *dominate over* current direct detection constraints.

B. Accelerating within its trapped region

We can refine the estimate in Equation (6) by observing that if a particle escapes its acceleration region, it no longer accumulates energy. i.e., the Larmor radius $r_L = E/(ZeB)$ needs to be smaller than the characteristic size of the source, L . Here, B is the magnetic field strength within the source, e the unit charge, and Z the charge number of the CR nucleus. This is called the *Hillas Criterion* [104]. As discussed in Refs. [99, 104–106] this is a *necessary* but not sufficient constraint on CR acceleration. Thus, we can treat it as a conservative scale. The criterion can be written as

$$E_{\text{CR}} < 10^{20} Z \left(\frac{B}{10 \mu\text{G}}\right) \left(\frac{L}{10 \text{kpc}}\right) \text{ eV}. \quad (7)$$

Note that this criterion can be improved by introducing flow velocities within the object [99, 105–107]. Here, we change the criterion to the following: *The particle's interaction length, $\lambda_{\chi,\text{CR}}$, needs to be larger than the Larmor-radius, r_L .* This is equivalent to requiring that the CR does not interact before escaping the acceleration site. Following [99] we define r_L as

$$r_L = 1.08 \frac{E}{Z B_{\mu\text{G}}} \text{ pc}, \quad (8)$$

where $B_{\mu\text{G}}$ is the magnetic field in micro-Gauss. To be conservative, we impose our criterion using the smallest Larmor radius imaginable at the source, namely that obtained with the magnetic field strength at the horizon of the SMBH. From observations, the magnetic field strength at the SMBH's horizon was estimated to be $B \sim 10^4$ G [108–110]. Thus, the Larmor radius for iron nuclei at the GZK cut-off in an AGN is

$$r_L \approx 2 \times 10^{-7} \text{ pc} \approx 6 \times 10^{11} \text{ cm}. \quad (9)$$

Note that r_L in Equation (9) is far smaller than the containment criterion in Equation (6) that used $r = 10^{-3}$ pc. On the other hand, the Larmor radius does not define *where* the acceleration of the CR happens. We set the acceleration site to 2×10^{-5} pc, which is larger than the maximum of $100R_S$ (for the MW) used in the modelling of AGNs [1–8]. We then require that the interaction length of Iron-DM is larger than the Larmor radius.

Another reason why this should be seen as a conservative bound is that it assumes the acceleration efficiency to be maximal, $\eta = 1$. As discussed in [111], η within these objects can be as low as $\eta \geq 0.03$. Note, other authors (e.g. [112]) describe this efficiency in terms of the acceleration time, t_{acc} . In general, it can be written as

$$t_{\text{acc}} = \mathcal{A} t_L, \quad (10)$$

with \mathcal{A} being a multiplier of the Larmor time t_L . In general, $\mathcal{A} \gg 1$ and in the specific case $\mathcal{A} \approx 1$, this corresponds to a maximally efficient acceleration process in a semi-relativistic scenario [112] (the assumption we are using here). In this scenario $t_{\text{acc}} \sim t_{\text{scattering}}$, where $t_{\text{scattering}}$ is the scattering time-scale. We now apply these criteria and the resulting bounds are

$$\sigma_{\chi, \text{CR}} \leq \begin{cases} 1 \times 10^{-22} \left(\frac{m_\chi}{\text{GeV}}\right) \text{ cm}^2 & \text{NFW}, \\ 7 \times 10^{-29} \left(\frac{m_\chi}{\text{GeV}}\right) \text{ cm}^2 & \text{Spike}, \end{cases} \quad (11)$$

improving the previous estimate. Note that the improvements are far smaller for an assumed NFW profile.

These bounds can now be further improved by assuming all CR are accelerated within an NGC1068-like galaxy, instead of a MW-like one. Plugging in the numbers from [13] (and $R_{\text{emission}} \leq 10^{-4}$ pc) we get a significant improvement of the bounds

$$\sigma_{\chi, \text{CR}} \leq 3 \times 10^{-31} \left(\frac{m_\chi}{\text{GeV}}\right) \text{ cm}^2. \quad (12)$$

C. Can the Cosmic Ray escape the galaxy?

Of note, is that [11] predict that the DM density rapidly falls for $r < 10R_S$ and vanishes completely for $r < 4R_S$. For Sagittarius A* with $M = 4 \times 10^6 M_\odot$ the Schwarzschild radius is 3.8×10^{-7} pc. Thus, CRs could be accelerated fully within a high-density shell of DM. This opens up the new question: *Does DM induce a GZK-like bound?* For simplicity, we alter this question and ask: *Does DM induce a high-energy cutoff for iron nuclei?* Since CR are accelerated within $100R_S < 2 \times 10^{-5}$ pc for a Milky-Way-like galaxy [1–8] ($< 1 \times 10^{-4}$ pc for NGC 1068), we can ask if an iron nucleus can pass through the DM halo without a single interaction. This results in an upper-bound on $\sigma_{\chi p}$ of

$$\sigma_{\chi, \text{CR}} \leq \begin{cases} 3 \times 10^{-24} \left(\frac{m_\chi}{\text{GeV}}\right) \text{ cm}^2 & \text{Burkert}, \\ 3 \times 10^{-26} \left(\frac{m_\chi}{\text{GeV}}\right) \text{ cm}^2 & \text{NFW}, \\ 9 \times 10^{-31} \left(\frac{m_\chi}{\text{GeV}}\right) \text{ cm}^2 & \text{MW – Spike}, \\ 1 \times 10^{-33} \left(\frac{m_\chi}{\text{GeV}}\right) \text{ cm}^2 & \text{NGC – Spike}. \end{cases} \quad (13)$$

This can be understood by comparing these numbers to the expectations from the GZK cut-off. For the GZK limit the photon-CR cross-section $\sigma_{\gamma p} \sim 3 \times 10^{-28}$ cm² is the relevant quantity [113]. The CMB density per cm³ is approximately 411 photons. This implies an interaction length of ~ 10 Mpc. Here the high DM densities scale the resulting cross-section for DM to lower values. For instance, the average density in a DM spike for a Milky-Way-like galaxy between 2×10^{-5} pc and 1 pc is $\sim 7 \times 10^9$ GeV/cm³.

Note, that the bound set by escape is stronger than the bound due to acceleration, mainly due to our conservative assumptions on the Larmor radius and acceleration time. Had we used smaller magnetic field strengths, the constraint from the trapped region would be stronger. For example, setting $B = 100$ G, results in $r_L \sim 4 \times 10^{-5}$ pc, similar in size to the assumed location of acceleration. This alone would yield a bound due to the acceleration criteria similar to the escape shown in Equation (13). If the acceleration were not 100% efficient, this would only further improve.

D. A non-conservative estimate

While in the previous sections, we used conservative estimates to derive bounds on DM-CR interactions, here we relax them: In NGC 1068 CRs can be accelerated as close as $\sim 10^{-5}$ pc from the central SMBH [13]. Additionally, as discussed previously, the efficiency of acceleration could be as low as $\eta = 0.03$ [111] (see [114] for even lower efficiencies). With these numbers $r_L \approx 1.3 \times 10^{-5}$ pc and $\rho_\chi^{\text{NGC}}(r = 10^{-5} \text{ pc}) \approx 5 \times 10^{18}$ GeV/cm³. In this scenario, the acceleration bound is the dominant contribution and the resulting constraint on the cross-section is $\sigma_{\chi, \text{CR}} \leq 8 \times 10^{-35} \frac{m_\chi}{\text{GeV}} \text{ cm}^2$.

E. Baryonic Feedback

Here we provide a rough estimate of baryonic feedback caused by the χ - p coupling on the formation of the spike. Baryonic feedback is relevant when DM has scattered at least once during the lifetime of the galactic DM halo, t_{age} . In that case, in order to avoid baryonic feedback, we can require that

$$t_{\text{age}} \times n_p \times v_p \times \sigma_{\chi p} \leq 1. \quad (14)$$

For illustration, we can use the age of the MW halo, $t_{\text{age}} \sim 10 \times 10^9$ years, the stellar mass density near Sagittarius A, $\rho_\odot \sim 3 \times 10^7 M_\odot \text{ pc}^{-3}$, and converting this criterion to a bound on the cross section, we obtain the approximate requirement that

$$\sigma_{\chi p} \leq 10^{-34} \text{ cm}^2 \quad (15)$$

to avoid feedback. The reasoning above assumes an isothermal core formation [115] (see also [116, 117]).

For larger cross sections (e.g., for most of the parameter space we target in the Milky-Way scenario), we assume the DM density profile follows the strong stellar heating scenario shown in Figure 2 and calculated in [48]. Figure 4 shows the resulting bounds including baryonic feedback. For the Milky Way scenario, this applies for all DM masses, while for the NGC 1068 case, masses ≥ 100 MeV are affected, which appears in our curves as a kink at about $m_\chi \sim 100$ MeV. We note that NGC1068

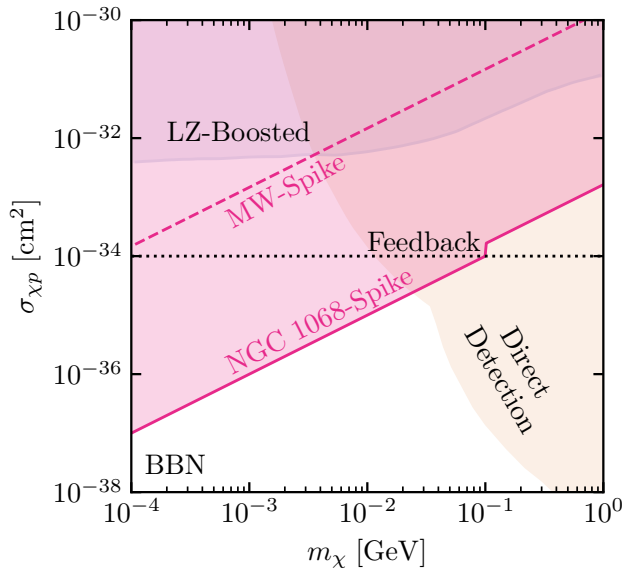


FIG. 3. The resulting bounds using the NFW and Spike profiles for the Milky-Way (marked MW) and assuming NGC1068-like population. These bounds are constructed under the assumption of a GZK-like process. The experimental bounds are from LZ [102]. Direct detection bounds adopted from [118] with bounds from CRESST [119, 120], DAMIC [121], DarkSide [122, 123], and XENON1T [124, 125]. BBN [126–128].

is significantly younger source, so the bound in Equation (15) will weaken accordingly.

Figure 3 shows the resulting bounds for spiked profiles, compared to current constraints.

F. A comment on TXS 0506+056

TXS 0506+056 was observed to be a source of neutrinos by Icecube [129]. Based on the neutrino and Gamma-Ray observations [130, 131], a few models predict that the main acceleration region of CR is $\mathcal{O}(\text{pc})$ away from the central SMBH [132–134], well outside of the possible DM spike. On the other hand, models exist where the production of neutrinos (thus the acceleration of CRs) happens between $4 \times 10^{-4} - 0.3 \text{ pc}$ [114, 135, 136]. Based on this, the spike profile has been used to constrain DM-neutrino interactions in those scenarios [137].

Setting the mass of the central SMBH to be $3 \times 10^8 M_{\odot}$ [138], the dark matter density will be between $10^{10} - 10^{15} \text{ GeV/cm}^3$ for the distances of interest. This is far. Assuming all high-energy (iron) CRs are accelerated within TXS-like objects, this would lead to a bound of $\sigma_{\chi, CR} \lesssim 10^{-33} \left(\frac{m_{\chi}}{\text{GeV}}\right) \text{ cm}^2$, when considering the CR should be able to escape the spike without interacting. This is similar to the NGC bound and is mainly due to the similar column densities between the two when considering escaping CRs.

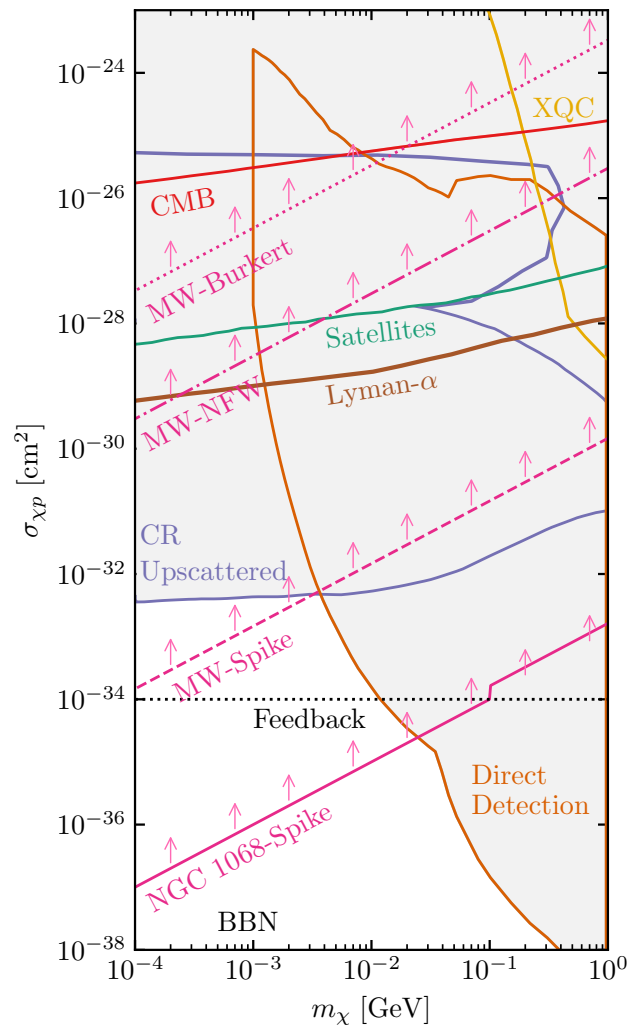


FIG. 4. The bounds for strongly interacting DM compared to current constraints. Current constraints are from XQC [139], CMB [140], Upscattered DM (LZ-Boosted [102] and PROSPECT [141]), EDELWEISS [142], CRESST 2017 (surface) [119, 143], XENON1T [124, 125, 144], CRESST-III [145, 146], DAMIC [121], DarkSide [122, 123], and XENON1T [124, 125]. BBN [126–128]. Milky-Way Satellites [103], Lyman- α [147], and re-interpretations of existing data [148].

V. CONCLUSION

Considering the recent spike in interest in spiky DM density profiles around supermassive black holes, it is very timely to find new observables to test the existence of such DM spikes. Conversely, it is also timely to ask what DM properties can be constrained in the presence of such spikes. In this work, we have introduced a novel method to constrain the DM-nucleon cross section within the spikes under various assumptions. We noted that relatively weak interactions between DM and SM baryons has the potential to disrupt the acceleration of ultra-

high-energy CRs in dense environments near supermassive black holes. This is the case even after accounting for baryonic feedback that can suppress DM spikes.

To set bounds on the values of these cross sections or make statements on the existence of DM spikes, we relied on a couple of assumptions. The first, and most crucial, is that CRs, particularly the heaviest elements like iron nuclei, are accelerated within DM spikes surrounding active galactic nuclei. If that is the case, they would fragment before reaching observed ultra-high energies, for sufficiently large $\sigma_{\chi p}$. By requiring that iron nuclei with energies ~ 50 EeV can be accelerated and escape without shattering, we derived conservative upper bounds on the DM–proton cross section. For a spiked DM profile in a Milky-Way-like galaxy, we obtained $\sigma_{\chi p} \lesssim 7 \times 10^{-29} (m_\chi/\text{GeV})\text{cm}^2$, improving to $\sigma_{\chi p} \lesssim 9 \times 10^{-31} (m_\chi/\text{GeV})\text{cm}^2$ when accounting for acceleration region geometry. We also examined whether DM could induce a GZK-like cut-off for iron nuclei within the AGN itself. From this, we set a bound on the DM–proton scattering cross section of $\sigma_{\chi\gamma} \lesssim 9 \times 10^{-31} (m_\chi/\text{GeV})\text{cm}^2$ assuming a spiked profile for MW-like galaxies and $\sigma_{\chi\gamma} \lesssim 1 \times 10^{-33} (m_\chi/\text{GeV})\text{cm}^2$ for NGC 1068-like galaxies.

These bounds probe DM interactions at momentum transfers $\gtrsim 10$ MeV, offering complementary and in some cases stronger constraints than those from direct detection or cosmological observations. In addition, given the large momentum transfers probed in this system, our bounds are also relevant to inelastic dark matter scenarios [149], where the interactions of DM particles with nucleons are necessarily inelastic, requiring a minimum amount of momentum exchange to produce the excited DM state, $\chi p \rightarrow \chi^* p$. These scenarios are much less constrained by direct detection experiments, though model-dependent limits from accelerators also apply [150, 151] (see also [51]). Our results demonstrate that ultra-high-energy CR survival and multi-messenger signatures from AGNs can provide powerful and model-independent constraints on DM. We emphasize that more robust and improved limits can be obtained by incorporating dark matter spikes in more detailed CR acceleration models and studying the energy dependence of the composition of CRs as observed at Earth.

ACKNOWLEDGMENTS

We are grateful for helpful discussions with Chris Cappiello, Dibya Chattopadhyay, Peter Cox, Raj Gandhi, Avirup Ghosh, Jayden Newstead and Yago Porto. This work was supported by the Australian Research Council through Discovery Project DP220101727 plus the University of Melbourne’s Research Computing Services and the Petascale Campus Initiative. This work was par-

tially supported by the University of Iowa’s Year 2 P3 Strategic Initiatives Program through funding received for the project entitled “High Impact Hiring Initiative (HIHI): A Program to Strategically Recruit and Retain Talented Faculty.” The work of B.D. was partly supported by the US Department of Energy under grant No. DE-SC0017987 and by a Humboldt Fellowship from the Alexander von Humboldt Foundation. S.A.M. and B.D. wish to acknowledge the Center for Theoretical Underground Physics and Related Areas (CETUP*) and the Institute for Underground Science at SURF for hospitality and for providing a stimulating environment, where a part of this work was done. B.D. also thanks the organizers of WHEPP 2025 at IIT, Hyderabad for local hospitality during the final stages of this work.

Appendix A: Is there a spike?

The existence of a DM spike is not well established in the literature, see for example [59, 152, 153]. Specifically, one of the mechanisms for the destruction of DM spikes are (galactic) mergers. During such mergers, the spike can be tidally disrupted reducing the density and consequently γ_{sp} . On the other hand [154] argue that specifically for the Milky Way, this destruction mechanism is unlikely, mainly due to the fact that the center of the Milky Way is believed to have formed 12 billion years ago in a single merger, without subsequent ones.

Another option for the suppression of the spike is stellar heating and dynamical friction [155]. While the DM spike is partially argued to exist due to the steeply rising stellar density near the GC, these stars could in turn lower the density via kinetic heating and capture. These processes would shift the expected $\gamma_{\text{sp}} \sim 7/3$ to $3/2$. While this is above the value predicted by the NFW profile, it is below the adiabatic prediction. Of note, is that observationally, there are claims that $\gamma \sim 2.3$ [156], which would be closer to a purely adiabatic regime. There are also suggestions, that the growth could happen instantaneously, not adiabatically. In such a scenario, while there would be a spike, it would be “blunted” compared to the adiabatic regime [59]. We note that even though stellar heating could suppress the spike [157], even in the maximal heating scenario, the DM density is still well above the predictions of a pure NFW profile.

The main problem with the spiked profile is the Core-Cusp problem. The prediction of the spike builds on a cuspy (NFW) profile. Some measurements seem to show that the DM density is more cored, which would significantly reduce the DM spike. However, there are no measurements below kpc-scale to distinguish a spike profile from a cored one. Additionally, the MW may be cored [43, 158, 159].

* stephan-meighen-berger@uiowa.edu

† bdev@wustl.edu

- ‡ matheus-hostert@uiowa.edu
- [1] K. Ptitsyna and A. Neronov, Particle acceleration in the vacuum gaps in black hole magnetospheres, *Astron. Astrophys.* **593**, A8 (2016), [arXiv:1510.04023 \[astro-ph.HE\]](https://arxiv.org/abs/1510.04023).
 - [2] Y. Inoue, D. Khangulyan, and A. Doi, On the Origin of High-energy Neutrinos from NGC 1068: The Role of Nonthermal Coronal Activity, *Astrophys. J. Lett.* **891**, L33 (2020), [arXiv:1909.02239 \[astro-ph.HE\]](https://arxiv.org/abs/1909.02239).
 - [3] K. Murase, S. S. Kimura, and P. Meszaros, Hidden Cores of Active Galactic Nuclei as the Origin of Medium-Energy Neutrinos: Critical Tests with the MeV Gamma-Ray Connection, *Phys. Rev. Lett.* **125**, 011101 (2020), [arXiv:1904.04226 \[astro-ph.HE\]](https://arxiv.org/abs/1904.04226).
 - [4] G. Katsoulakos and F. M. Rieger, Gap-type Particle Acceleration in the Magnetospheres of Rotating Supermassive Black Holes, *Astrophys. J.* **895**, 99 (2020), [arXiv:2005.05076 \[astro-ph.HE\]](https://arxiv.org/abs/2005.05076).
 - [5] A. Kheirandish, K. Murase, and S. S. Kimura, High-energy Neutrinos from Magnetized Coronae of Active Galactic Nuclei and Prospects for Identification of Seyfert Galaxies and Quasars in Neutrino Telescopes, *Astrophys. J.* **922**, 45 (2021), [arXiv:2102.04475 \[astro-ph.HE\]](https://arxiv.org/abs/2102.04475).
 - [6] B. Eichmann, F. Oikonomou, S. Salvatore, R.-J. Dettmar, and J. Becker Tjus, Solving the Multimessenger Puzzle of the AGN-starburst Composite Galaxy NGC 1068, *Astrophys. J.* **939**, 43 (2022), [arXiv:2207.00102 \[astro-ph.HE\]](https://arxiv.org/abs/2207.00102).
 - [7] S. Inoue, M. Cerruti, K. Murase, and R.-Y. Liu, Multimessenger emission from winds and tori in active galactic nuclei, *PoS ICRC2023*, 1161 (2023), [arXiv:2207.02097 \[astro-ph.HE\]](https://arxiv.org/abs/2207.02097).
 - [8] D. F. G. Fiorillo, L. Comisso, E. Peretti, M. Petropoulou, and L. Sironi, A Magnetized Strongly Turbulent Corona as the Source of Neutrinos from NGC 1068, *Astrophys. J.* **974**, 75 (2024), [arXiv:2407.01678 \[astro-ph.HE\]](https://arxiv.org/abs/2407.01678).
 - [9] R. Abbasi *et al.* (IceCube), Evidence for neutrino emission from the nearby active galaxy NGC 1068, *Science* **378**, 538 (2022), [arXiv:2211.09972 \[astro-ph.HE\]](https://arxiv.org/abs/2211.09972).
 - [10] P. Padovani *et al.*, High-energy neutrinos from the vicinity of the supermassive black hole in NGC 1068, *Nature Astron.* **8**, 1077 (2024), [arXiv:2405.20146 \[astro-ph.HE\]](https://arxiv.org/abs/2405.20146).
 - [11] P. Gondolo and J. Silk, Dark matter annihilation at the galactic center, *Phys. Rev. Lett.* **83**, 1719 (1999), [arXiv:astro-ph/9906391](https://arxiv.org/abs/astro-ph/9906391).
 - [12] C. V. Capiello, K. C. Y. Ng, and J. F. Beacom, Reverse Direct Detection: Cosmic Ray Scattering With Light Dark Matter, *Phys. Rev. D* **99**, 063004 (2019), [arXiv:1810.07705 \[hep-ph\]](https://arxiv.org/abs/1810.07705).
 - [13] G. Herrera and K. Murase, Probing light dark matter through cosmic-ray cooling in active galactic nuclei, *Phys. Rev. D* **110**, L011701 (2024), [arXiv:2307.09460 \[hep-ph\]](https://arxiv.org/abs/2307.09460).
 - [14] G. Elor, R. McGehee, and A. Pierce, Maximizing Direct Detection with Highly Interactive Particle Relic Dark Matter, *Phys. Rev. Lett.* **130**, 031803 (2023), [arXiv:2112.03920 \[hep-ph\]](https://arxiv.org/abs/2112.03920).
 - [15] P. N. Bhattiprolu, G. Elor, R. McGehee, and A. Pierce, Freezing-in hadrophilic dark matter at low reheating temperatures, *JHEP* **01**, 128, [arXiv:2210.15653 \[hep-ph\]](https://arxiv.org/abs/2210.15653).
 - [16] A. Burkert, The Structure of dark matter halos in dwarf galaxies, *Astrophys. J. Lett.* **447**, L25 (1995), [arXiv:astro-ph/9504041](https://arxiv.org/abs/astro-ph/9504041).
 - [17] J. F. Navarro, C. S. Frenk, and S. D. M. White, The Structure of cold dark matter halos, *Astrophys. J.* **462**, 563 (1996), [arXiv:astro-ph/9508025](https://arxiv.org/abs/astro-ph/9508025).
 - [18] D. Berge *et al.*, Fast variability of TeV gamma-rays from the radio galaxy M87, *Science* **314**, 1424 (2006), [arXiv:astro-ph/0612016](https://arxiv.org/abs/astro-ph/0612016).
 - [19] F. Aharonian *et al.*, An Exceptional Very High Energy Gamma-Ray Flare of PKS 2155-304, *Astrophys. J. Lett.* **664**, L71 (2007), [arXiv:0706.0797 \[astro-ph\]](https://arxiv.org/abs/0706.0797).
 - [20] V. A. Acciari *et al.*, Observation of gamma-ray emission from the galaxy M87 above 250 GeV with VERITAS, *Astrophys. J.* **679**, 397 (2008), [arXiv:0802.1951 \[astro-ph\]](https://arxiv.org/abs/0802.1951).
 - [21] A. Abramowski *et al.* (H.E.S.S., VERITAS), The 2010 very high energy gamma-ray flare & 10 years of multi-wavelength observations of M 87, *Astrophys. J.* **746**, 151 (2012), [arXiv:1111.5341 \[astro-ph.CO\]](https://arxiv.org/abs/1111.5341).
 - [22] J. Aleksic *et al.* (MAGIC), MAGIC observations of the giant radio galaxy M87 in a low-emission state between 2005 and 2007, *Astron. Astrophys.* **544**, A96 (2012), [arXiv:1207.2147 \[astro-ph.HE\]](https://arxiv.org/abs/1207.2147).
 - [23] J. Aleksic *et al.*, Black hole lightning due to particle acceleration at subhorizon scales, *Science* **346**, 1080 (2014), [arXiv:1412.4936 \[astro-ph.HE\]](https://arxiv.org/abs/1412.4936).
 - [24] V. S. Berezinsky, in *Proceedings of the International Conference Neutrino '77* (1977) p. 177.
 - [25] D. Eichler, HIGH-ENERGY NEUTRINO ASTRONOMY: A PROBE OF GALACTIC NUCLEI?, *Astrophys. J.* **232**, 106 (1979).
 - [26] R. Silberberg and M. M. Shapiro, NEUTRINOS AS A PROBE FOR THE NATURE OF AND PROCESSES IN ACTIVE GALACTIC NUCLEI., in *16th International Cosmic Ray Conference* (1979) pp. 357–362.
 - [27] R. C. Hickox and D. M. Alexander, Obscured Active Galactic Nuclei, *Ann. Rev. Astron. Astrophys.* **56**, 625 (2018), [arXiv:1806.04680 \[astro-ph.GA\]](https://arxiv.org/abs/1806.04680).
 - [28] R. Abbasi *et al.* (IceCube), Search for neutrino emission from cores of active galactic nuclei, *Phys. Rev. D* **106**, 022005 (2022), [arXiv:2111.10169 \[astro-ph.HE\]](https://arxiv.org/abs/2111.10169).
 - [29] P. Giommi and P. Padovani, Astrophysical Neutrinos and Blazars, *Universe* **7**, 492 (2021), [arXiv:2112.06232 \[astro-ph.HE\]](https://arxiv.org/abs/2112.06232).
 - [30] K. Fang, J. S. Gallagher, and F. Halzen, The TeV Diffuse Cosmic Neutrino Spectrum and the Nature of Astrophysical Neutrino Sources, *Astrophys. J.* **933**, 190 (2022), [arXiv:2205.03740 \[astro-ph.HE\]](https://arxiv.org/abs/2205.03740).
 - [31] G. Setti and L. Woltjer, Active galactic nuclei and the spectrum of the x-ray background, *Astronomy and Astrophysics (ISSN 0004-6361)*, vol. 224, no. 1-2, Oct. 1989, p. L21-L23. **224**, L21 (1989).
 - [32] A. Comastri, G. Setti, G. Zamorani, and G. Hasinger, The Contribution of AGNs to the x-ray background, *Astron. Astrophys.* **296**, 1 (1995), [arXiv:astro-ph/9409067](https://arxiv.org/abs/astro-ph/9409067).
 - [33] E. Treister and C. M. Urry, The Evolution of Obscuration in AGN, *Astrophys. J. Lett.* **652**, L79 (2006), [arXiv:astro-ph/0610525](https://arxiv.org/abs/astro-ph/0610525).
 - [34] A. Akylas, A. Georgakakis, I. Georgantopoulos, M. Brightman, and K. Nandra, Constraining the fraction of Compton-thick AGN in the Universe by modelling the diffuse X-ray background spectrum, *Astron. Astrophys.* **546**, A98 (2012), [arXiv:1209.5398 \[astro-](https://arxiv.org/abs/1209.5398)

- ph.HE].
- [35] T. T. Ananna, E. Treister, C. M. Urry, C. Ricci, A. Kirkpatrick, S. LaMassa, J. Buchner, M. Tremmel, S. Marchesi, and F. Civano, The Accretion History of AGNs. I. Supermassive Black Hole Population Synthesis Model, *Astrophys. J.* **871**, 240 (2019), arXiv:1810.02298 [astro-ph.GA].
- [36] R. Gilli, A. Comastri, and G. Hasinger, The synthesis of the cosmic X-ray background in the Chandra and XMM-Newton era, *Astron. Astrophys.* **463**, 79 (2007), arXiv:astro-ph/0610939.
- [37] P. Padovani, R. Gilli, E. Resconi, C. Bellenghi, and F. Henningsen, The neutrino background from non-jetted active galactic nuclei, *Astron. Astrophys.* **684**, L21 (2024), arXiv:2404.05690 [astro-ph.HE].
- [38] Q.-R. Yang, X.-B. Chen, R.-Y. Liu, X.-Y. Wang, and M. Lemoine, On the origin of ~ 100 TeV neutrinos from the Seyfert galaxy NGC 7469 (2025), arXiv:2510.19662 [astro-ph.HE].
- [39] O. Y. Gnedin and J. R. Primack, Dark Matter Profile in the Galactic Center, *Phys. Rev. Lett.* **93**, 061302 (2004), arXiv:astro-ph/0308385.
- [40] M. Portail, C. Wegg, O. Gerhard, and I. Martinez-Valpuesta, Made-to-measure models of the galactic box/peanut bulge: stellar and total mass in the bulge region, *Monthly Notices of the Royal Astronomical Society* **448**, 713 (2015), <https://academic.oup.com/mnras/article-pdf/448/1/713/9389491/stv058.pdf>.
- [41] F. Iocco and M. Benito, An estimate of the DM profile in the Galactic bulge region, *Physics of the Dark Universe* **15**, 90 (2017), arXiv:1611.09861 [astro-ph.GA].
- [42] D. Hooper, The Density of Dark Matter in the Galactic Bulge and Implications for Indirect Detection, *Phys. Dark Univ.* **15**, 53 (2017), arXiv:1608.00003 [astro-ph.HE].
- [43] M. Baumgart, S. Bottaro, D. Redigolo, N. L. Rodd, and T. R. Slatyer, Testing Real WIMPs with CTAO, (2025), arXiv:2507.15937 [hep-ph].
- [44] G. D. Quinlan, L. Hernquist, and S. Sigurdsson, Models of Galaxies with Central Black Holes: Adiabatic Growth in Spherical Galaxies, *Astrophys. J.* **440**, 554 (1995), arXiv:astro-ph/9407005.
- [45] L. Sadeghian, F. Ferrer, and C. M. Will, Dark matter distributions around massive black holes: A general relativistic analysis, *Phys. Rev. D* **88**, 063522 (2013), arXiv:1305.2619 [astro-ph.GA].
- [46] P. Sandick, J. Diemand, K. Freese, and D. Spolyar, Black Holes in our Galactic Halo: Compatibility with FGST and PAMELA Data and Constraints on the First Stars, *JCAP* **01**, 018, arXiv:1008.3552 [astro-ph.CO].
- [47] M. Regis and P. Ullio, Multi-wavelength signals of dark matter annihilations at the Galactic center, *Phys. Rev. D* **78**, 043505 (2008), arXiv:0802.0234 [hep-ph].
- [48] S. Balaji, D. Sachdeva, F. Sala, and J. Silk, Dark matter spikes around Sgr A* in γ -rays, *JCAP* **08**, 063, arXiv:2303.12107 [hep-ph].
- [49] T. Lacroix, Dynamical constraints on a dark matter spike at the Galactic Centre from stellar orbits, *Astron. Astrophys.* **619**, A46 (2018), arXiv:1801.01308 [astro-ph.GA].
- [50] R. A. Gustafson, I. M. Shoemaker, and V. Takhistov, Probing Dark Matter Interactions with Stellar Motion near Sagittarius A* (2025), arXiv:2510.07387 [hep-ph].
- [51] J. F. Acevedo, A. J. Reilly, and L. Santos-Olmsted, Dark Drag Around Sagittarius A* (2025), arXiv:2510.01320 [hep-ph].
- [52] I. John, R. K. Leane, and T. Linden, Dark matter scattering constraints from observations of stars surrounding Sgr A*, *Phys. Rev. D* **109**, 123041 (2024), arXiv:2311.16228 [astro-ph.HE].
- [53] B. Betancourt Kamenetskaia, *Observable signatures and consequences of high-density dark matter environments*, Ph.D. thesis, Munich, Tech U. (2025).
- [54] K. Akita, A. Ibarra, and R. Zimmermann, Dark matter explanations for the neutrino emission from the Seyfert galaxy NGC 1068 (2025), arXiv:2507.16539 [hep-ph].
- [55] J. M. Cline, S. Gao, F. Guo, Z. Lin, S. Liu, M. Puel, P. Todd, and T. Xiao, Blazar Constraints on Neutrino-Dark Matter Scattering, *Phys. Rev. Lett.* **130**, 091402 (2023), arXiv:2209.02713 [hep-ph].
- [56] F. Ferrer, G. Herrera, and A. Ibarra, New constraints on the dark matter-neutrino and dark matter-photon scattering cross sections from TXS 0506+056, *JCAP* **05**, 057, arXiv:2209.06339 [hep-ph].
- [57] J. M. Cline and M. Puel, NGC 1068 constraints on neutrino-dark matter scattering, *JCAP* **06**, 004, arXiv:2301.08756 [hep-ph].
- [58] P. S. B. Dev, D. Kim, D. Sathyan, K. Sinha, and Y. Zhang, New Constraints on Neutrino-Dark Matter Interactions: A Comprehensive Analysis (2025), arXiv:2507.01000 [hep-ph].
- [59] P. Ullio, H. Zhao, and M. Kamionkowski, A Dark matter spike at the galactic center?, *Phys. Rev. D* **64**, 043504 (2001), arXiv:astro-ph/0101481.
- [60] Z.-Q. Shen, G.-W. Yuan, C.-Z. Jiang, Y.-L. S. Tsai, Q. Yuan, and Y.-Z. Fan, Exploring dark matter spike distribution around the Galactic centre with stellar orbits, *Mon. Not. Roy. Astron. Soc.* **527**, 3196 (2023), arXiv:2303.09284 [astro-ph.GA].
- [61] T. K. Gaisser, Spectrum of cosmic-ray nucleons, kaon production, and the atmospheric muon charge ratio, *Astropart. Phys.* **35**, 801 (2012), arXiv:1111.6675 [astro-ph.HE].
- [62] S. Thoudam, J. P. Rachen, A. van Vliet, A. Achterberg, S. Buitink, H. Falcke, and J. R. Hörandel, Cosmic-ray energy spectrum and composition up to the ankle: the case for a second Galactic component, *Astron. Astrophys.* **595**, A33 (2016), arXiv:1605.03111 [astro-ph.HE].
- [63] M. S. Muzio, M. Unger, and G. R. Farrar, Progress towards characterizing ultrahigh energy cosmic ray sources, *Phys. Rev. D* **100**, 103008 (2019), arXiv:1906.06233 [astro-ph.HE].
- [64] D. Ivanov (Telescope Array), Energy Spectrum Measured by the Telescope Array, *PoS ICRC2019*, 298 (2020).
- [65] E. W. Mayotte *et al.* (Pierre Auger), Measurement of the mass composition of ultra-high-energy cosmic rays at the Pierre Auger Observatory, *PoS ICRC2023*, 365 (2023).
- [66] D. Ehlert, A. van Vliet, F. Oikonomou, and W. Winter, Constraints on the proton fraction of cosmic rays at the highest energies and the consequences for cosmogenic neutrinos and photons, *JCAP* **02**, 022, arXiv:2304.07321 [astro-ph.HE].
- [67] B. T. Zhang, K. Murase, N. Ekanger, M. Bhattacharya, and S. Horiuchi, Ultraheavy Ultrahigh-Energy Cosmic Rays (2024), arXiv:2405.17409 [astro-ph.HE].

- [68] R. U. Abbasi *et al.* (Telescope Array), Isotropy of Cosmic Rays beyond 1020 eV Favors Their Heavy Mass Composition, *Phys. Rev. Lett.* **133**, 041001 (2024), [arXiv:2406.19287 \[astro-ph.HE\]](#).
- [69] R. Abbasi *et al.* ((IceCube Collaboration)§, IceCube), Search for Extremely-High-Energy Neutrinos and First Constraints on the Ultrahigh-Energy Cosmic-Ray Proton Fraction with IceCube, *Phys. Rev. Lett.* **135**, 031001 (2025), [arXiv:2502.01963 \[astro-ph.HE\]](#).
- [70] A. Abdul Halim *et al.* (Pierre Auger), Energy Spectrum of Ultrahigh-Energy Cosmic Rays across Declinations -90° to $+44.8^\circ$ as Measured at the Pierre Auger Observatory, *Phys. Rev. Lett.* **135**, 241002 (2025), [arXiv:2506.11688 \[astro-ph.HE\]](#).
- [71] R. Abbasi *et al.* (IceCube), Measurement of the mean number of muons with energies above 500 GeV in air showers detected with the IceCube Neutrino Observatory (2025), [arXiv:2506.19241 \[hep-ex\]](#).
- [72] K. Greisen, End to the cosmic ray spectrum?, *Phys. Rev. Lett.* **16**, 748 (1966).
- [73] G. T. Zatsepin and V. A. Kuzmin, Upper limit of the spectrum of cosmic rays, *JETP Lett.* **4**, 78 (1966).
- [74] D. J. Bird *et al.* (HIRES), Detection of a cosmic ray with measured energy well beyond the expected spectral cutoff due to cosmic microwave radiation, *Astrophys. J.* **441**, 144 (1995), [arXiv:astro-ph/9410067](#).
- [75] A. Abdul Halim *et al.* (Pierre Auger), A Catalog of the Highest-Energy Cosmic Rays Recorded during Phase I of Operation of the Pierre Auger Observatory, *Astrophys. J. Suppl.* **264**, 50 (2023), [arXiv:2211.16020 \[astro-ph.HE\]](#).
- [76] R. U. Abbasi *et al.* (Telescope Array), An extremely energetic cosmic ray observed by a surface detector array, *Science* **382**, abo5095 (2023), [arXiv:2311.14231 \[astro-ph.HE\]](#).
- [77] A. Aab *et al.* (Pierre Auger), Measurement of the cosmic-ray energy spectrum above 2.5×10^{18} eV using the Pierre Auger Observatory, *Phys. Rev. D* **102**, 062005 (2020), [arXiv:2008.06486 \[astro-ph.HE\]](#).
- [78] K. Lu, Y.-L. S. Tsai, Q. Yuan, and L. Zhang, Inelastic Scattering of Dark Matter with Heavy Cosmic Rays, *Res. Astron. Astrophys.* **24**, 065007 (2024), [arXiv:2310.12501 \[astro-ph.HE\]](#).
- [79] M. Aguilar *et al.* (AMS), Properties of Iron Primary Cosmic Rays: Results from the Alpha Magnetic Spectrometer, *Phys. Rev. Lett.* **126**, 041104 (2021).
- [80] M. Froissart, Asymptotic behavior and subtractions in the Mandelstam representation, *Phys. Rev.* **123**, 1053 (1961).
- [81] A. Martin, Unitarity and high-energy behavior of scattering amplitudes, *Phys. Rev.* **129**, 1432 (1963).
- [82] R. J. Glauber and G. Matthiae, High-energy scattering of protons by nuclei, *Nucl. Phys. B* **21**, 135 (1970).
- [83] M. M. Block and F. Halzen, New evidence for the saturation of the Froissart bound, *Phys. Rev. D* **72**, 036006 (2005), [Erratum: *Phys. Rev. D* **72**, 039902 (2005)], [arXiv:hep-ph/0506031](#).
- [84] R. Ulrich, R. Engel, and M. Unger, Hadronic Multiparticle Production at Ultra-High Energies and Extensive Air Showers, *Phys. Rev. D* **83**, 054026 (2011), [arXiv:1010.4310 \[hep-ph\]](#).
- [85] T. K. Gaisser, T. Stanev, and S. Tilav, Cosmic Ray Energy Spectrum from Measurements of Air Showers, *Front. Phys. (Beijing)* **8**, 748 (2013), [arXiv:1303.3565 \[astro-ph.HE\]](#).
- [86] G. Bertone and D. Merritt, Time-dependent models for dark matter at the Galactic Center, *Phys. Rev. D* **72**, 103502 (2005), [arXiv:astro-ph/0501555](#).
- [87] G. Bertone and D. Merritt, Dark matter dynamics and indirect detection, *Mod. Phys. Lett. A* **20**, 1021 (2005), [arXiv:astro-ph/0504422](#).
- [88] F. Ferrer, A. M. da Rosa, and C. M. Will, Dark matter spikes in the vicinity of Kerr black holes, *Phys. Rev. D* **96**, 083014 (2017), [arXiv:1707.06302 \[astro-ph.CO\]](#).
- [89] R. Abuter *et al.* (GRAVITY), Polarimetry and astrometry of NIR flares as event horizon scale, dynamical probes for the mass of Sgr A*, *Astron. Astrophys.* **677**, L10 (2023), [arXiv:2307.11821 \[astro-ph.GA\]](#).
- [90] G. Lodato and G. Bertin, Non-Keplerian rotation in the nucleus of NGC 1068: Evidence for a massive accretion disk?, *Astron. Astrophys.* **398**, 517 (2003), [arXiv:astro-ph/0211113](#).
- [91] J.-H. Woo and C. M. Urry, AGN black hole masses and bolometric luminosities, *Astrophys. J.* **579**, 530 (2002), [arXiv:astro-ph/0207249](#).
- [92] E. Dalla Bontà, B. M. Peterson, C. J. Grier, M. Berton, W. N. Brandt, S. Ciroti, E. M. Corsini, B. Dalla Barba, R. Davies, M. Dehghanian, R. Edelson, L. Foschini, D. Gasparri, L. C. Ho, K. Horne, E. Iodice, L. Morelli, A. Pizzella, E. Portaluri, Y. Shen, D. P. Schneider, and M. Vestergaard, Estimating masses of supermassive black holes in active galactic nuclei from the $h\alpha$ emission line, *Astronomy & Astrophysics* **696**, A48 (2025).
- [93] T. Bringmann and M. Pospelov, Novel direct detection constraints on light dark matter, *Phys. Rev. Lett.* **122**, 171801 (2019), [arXiv:1810.10543 \[hep-ph\]](#).
- [94] J. B. Dent, B. Dutta, J. L. Newstead, and I. M. Shoemaker, Bounds on Cosmic Ray-Boosted Dark Matter in Simplified Models and its Corresponding Neutrino-Floor, *Phys. Rev. D* **101**, 116007 (2020), [arXiv:1907.03782 \[hep-ph\]](#).
- [95] M. Císcar-Monsalvatje, G. Herrera, and I. M. Shoemaker, Upper limits on the cosmic neutrino background from cosmic rays, *Phys. Rev. D* **110**, 063036 (2024), [arXiv:2402.00985 \[hep-ph\]](#).
- [96] D. Bardhan, S. Bhowmick, D. Ghosh, A. Guha, and D. Sachdeva, Bounds on boosted dark matter from direct detection: The role of energy-dependent cross sections, *Phys. Rev. D* **107**, 015010 (2023), [arXiv:2208.09405 \[hep-ph\]](#).
- [97] J. Zhang, A. Sandrock, J. Liao, and B. Yue, Impact of coherent scattering on relic neutrinos boosted by cosmic rays (2025), [arXiv:2505.04791 \[hep-ph\]](#).
- [98] F. M. Rieger, UHE Cosmic Rays and AGN Jets, *PoS HEPROVII*, 019 (2020), [arXiv:1911.04171 \[astro-ph.HE\]](#).
- [99] F. M. Rieger, Active Galactic Nuclei as Potential Sources of Ultra-High Energy Cosmic Rays, *Universe* **8**, 607 (2022), [arXiv:2211.12202 \[astro-ph.HE\]](#).
- [100] V. K. Jha, R. Joshi, H. Chand, X.-B. Wu, L. C. Ho, S. Rastogi, and Q. Ma, Accretion disc sizes from continuum reverberation mapping of AGN selected from the ZTF survey, *Monthly Notices of the Royal Astronomical Society* **511**, 3005 (2022), [arXiv:2109.05036 \[astro-ph.GA\]](#).
- [101] W.-J. Guo, Y.-R. Li, Z.-X. Zhang, L. C. Ho, and J.-M. Wang, Accretion Disk Size Measurements of Active Galactic Nuclei Monitored by the Zwicky Transient Fa-

- cility, *Astrophys. J.* **929**, 19 (2022), arXiv:2201.08533 [astro-ph.GA].
- [102] J. Aalbers *et al.* (LZ), New Constraints on Cosmic Ray-Boosted Dark Matter from the LUX-ZEPLIN Experiment, *Phys. Rev. Lett.* **134**, 241801 (2025), arXiv:2503.18158 [hep-ex].
- [103] E. O. Nadler, V. Gluscevic, K. K. Boddy, and R. H. Wechsler, Constraints on Dark Matter Microphysics from the Milky Way Satellite Population, *Astrophys. J. Lett.* **878**, 32 (2019), [Erratum: *Astrophys. J. Lett.* 897, L46 (2020), Erratum: *Astrophys. J.* 897, L46 (2020)], arXiv:1904.10000 [astro-ph.CO].
- [104] A. M. Hillas, The Origin of Ultrahigh-Energy Cosmic Rays, *Ann. Rev. Astron. Astrophys.* **22**, 425 (1984).
- [105] K. V. Ptitsyna and S. V. Troitsky, Physical conditions in potential sources of ultra-high-energy cosmic rays. I. Updated Hillas plot and radiation-loss constraints, *Phys. Usp.* **53**, 691 (2010), arXiv:0808.0367 [astro-ph].
- [106] K. Kotera and A. V. Olinto, The Astrophysics of Ultrahigh Energy Cosmic Rays, *Ann. Rev. Astron. Astrophys.* **49**, 119 (2011), arXiv:1101.4256 [astro-ph.HE].
- [107] A. R. Bell, Cosmic ray acceleration, *Astropart. Phys.* **43**, 56 (2013).
- [108] N. A. Silant'ev, M. Y. Piotrovich, Y. N. Gnedin, and T. M. Natsvlshvili, Magnetic fields of AGNs and standard accretion disk model: testing by optical polarimetry, *A&A* **507**, 171 (2009), arXiv:0909.1207 [astro-ph.CO].
- [109] A. K. Baczkó *et al.*, A Highly Magnetized Twin-Jet Base Pinpoints a Supermassive Black Hole, *Astron. Astrophys.* **593**, A47 (2016), arXiv:1605.07100 [astro-ph.GA].
- [110] M. Y. Piotrovich, A. G. Mikhailov, S. D. Buliga, and T. M. Natsvlshvili, Determination of magnetic field strength on the event horizon of supermassive black holes in active galactic nuclei, *Mon. Not. Roy. Astron. Soc.* **495**, 614 (2020), arXiv:2004.07075 [astro-ph.HE].
- [111] F. A. Aharonian, A. A. Belyanin, E. V. Derishev, V. V. Kocharovsky, and V. V. Kocharovsky, Constraints on the extremely high-energy cosmic ray accelerators from classical electrodynamics, *Phys. Rev. D* **66**, 023005 (2002), arXiv:astro-ph/0202229.
- [112] M. Lemoine and E. Waxman, Anisotropy vs chemical composition at ultra-high energies, *Journal of Cosmology and Astroparticle Physics* **2009** (11), 009, arXiv:0907.1354 [astro-ph.HE].
- [113] A. A. Arkhipov, The GZK puzzle and fundamental dynamics (2006), arXiv:hep-ph/0607265.
- [114] Q.-R. Yang, R.-Y. Liu, and X.-Y. Wang, Could the Neutrino Emission of TXS 0506+056 Come from the Accretion Flow of the Supermassive Black Hole?, *Astrophys. J.* **980**, 255 (2025), arXiv:2411.17632 [astro-ph.HE].
- [115] B. Betancourt Kamenetskaia, M. Fujiwara, A. Ibarra, and T. Toma, Dark matter spikes with strongly self-interacting particles (2025), arXiv:2506.12642 [hep-ph].
- [116] D. N. Spergel and P. J. Steinhardt, Observational evidence for selfinteracting cold dark matter, *Phys. Rev. Lett.* **84**, 3760 (2000), arXiv:astro-ph/9909386.
- [117] M. Kaplinghat, S. Tulin, and H.-B. Yu, Dark Matter Halos as Particle Colliders: Unified Solution to Small-Scale Structure Puzzles from Dwarfs to Clusters, *Phys. Rev. Lett.* **116**, 041302 (2016), arXiv:1508.03339 [astro-ph.CO].
- [118] J. Billard *et al.*, Direct detection of dark matter—APPEC committee report*, *Rept. Prog. Phys.* **85**, 056201 (2022), arXiv:2104.07634 [hep-ex].
- [119] G. Angloher *et al.* (CRESST), Results on MeV-scale dark matter from a gram-scale cryogenic calorimeter operated above ground, *Eur. Phys. J. C* **77**, 637 (2017), arXiv:1707.06749 [astro-ph.CO].
- [120] G. Angloher *et al.* (CRESST), Testing spin-dependent dark matter interactions with lithium aluminate targets in CRESST-III, *Phys. Rev. D* **106**, 092008 (2022), arXiv:2207.07640 [astro-ph.CO].
- [121] A. Aguilar-Arevalo *et al.* (DAMIC), Results on low-mass weakly interacting massive particles from a 11 kg-day target exposure of DAMIC at SNOLAB, *Phys. Rev. Lett.* **125**, 241803 (2020), arXiv:2007.15622 [astro-ph.CO].
- [122] P. Agnes *et al.* (DarkSide), Low-Mass Dark Matter Search with the DarkSide-50 Experiment, *Phys. Rev. Lett.* **121**, 081307 (2018), arXiv:1802.06994 [astro-ph.HE].
- [123] P. Agnes *et al.* (DarkSide), DarkSide-50 532-day Dark Matter Search with Low-Radioactivity Argon, *Phys. Rev. D* **98**, 102006 (2018), arXiv:1802.07198 [astro-ph.CO].
- [124] E. Aprile *et al.* (XENON), Dark Matter Search Results from a One Ton-Year Exposure of XENON1T, *Phys. Rev. Lett.* **121**, 111302 (2018), arXiv:1805.12562 [astro-ph.CO].
- [125] E. Aprile *et al.* (XENON), Light Dark Matter Search with Ionization Signals in XENON1T, *Phys. Rev. Lett.* **123**, 251801 (2019), arXiv:1907.11485 [hep-ex].
- [126] N. Sabti, J. Alvey, M. Escudero, M. Fairbairn, and D. Blas, Refined Bounds on MeV-scale Thermal Dark Sectors from BBN and the CMB, *JCAP* **01**, 004, arXiv:1910.01649 [hep-ph].
- [127] G. Krnjaic and S. D. McDermott, Implications of BBN Bounds for Cosmic Ray Upscattered Dark Matter, *Phys. Rev. D* **101**, 123022 (2020), arXiv:1908.00007 [hep-ph].
- [128] N. Sabti, J. Alvey, M. Escudero, M. Fairbairn, and D. Blas, Addendum: Refined bounds on MeV-scale thermal dark sectors from BBN and the CMB, *JCAP* **08**, A01, arXiv:2107.11232 [hep-ph].
- [129] M. G. Aartsen *et al.* (IceCube), Neutrino emission from the direction of the blazar TXS 0506+056 prior to the IceCube-170922A alert, *Science* **361**, 147 (2018), arXiv:1807.08794 [astro-ph.HE].
- [130] Y. T. Tanaka, S. Buson, and D. Kocevski, Fermi-LAT detection of increased gamma-ray activity of TXS 0506+056, located inside the IceCube-170922A error region., *The Astronomer's Telegram* **10791**, 1 (2017).
- [131] S. Ansoldi *et al.* (MAGIC), The blazar TXS 0506+056 associated with a high-energy neutrino: insights into extragalactic jets and cosmic ray acceleration, *Astrophys. J. Lett.* **863**, L10 (2018), arXiv:1807.04300 [astro-ph.HE].
- [132] E. M. de Gouveia Dal Pino, J. C. Rodríguez-Ramírez, and M. V. del Valle, Multi-messenger emission from magnetic reconnection in blazar jets: the case of TXS 0506+056 (2024), arXiv:2411.10210 [astro-ph.HE].
- [133] E. Kun, P. L. Biermann, and L. 'A. Gergely, VLBI radio structure and radio brightening of the high-energy neutrino emitting blazar TXS 0506+056 (2018), arXiv:1807.07942 [astro-ph.HE].
- [134] A. Caproni, Z. Abraham, H. Monteiro, and et al., Relativistic parsec-scale jets of the blazars TXS 0506+056

- and PKS 0502+049 and their possible association with gamma-ray flares and neutrino production, *Mon. Not. Roy. Astron. Soc.* **509**, 1646 (2022), [arXiv:2111.01772 \[astro-ph.HE\]](#).
- [135] R. Xue, R.-Y. Liu, M. Petropoulou, F. Oikonomou, Z.-R. Wang, K. Wang, and X.-Y. Wang, A two-zone model for blazar emission: implications for TXS 0506+056 and the neutrino event IceCube-170922A (2019), [arXiv:1908.10190 \[astro-ph.HE\]](#).
- [136] R. Xue, R.-Y. Liu, Z.-R. Wang, N. Ding, and X.-Y. Wang, A Two-zone Blazar Radiation Model for “Orphan” Neutrino Flares, *Astrophys. J.* **906**, 51 (2021), [arXiv:2011.03681 \[astro-ph.HE\]](#).
- [137] G. D. Zapata, J. Jones-Pérez, and A. M. Gago, Bounds on neutrino-DM interactions from TXS 0506+056 neutrino outburst, *JCAP* **07**, 042, [arXiv:2503.03823 \[hep-ph\]](#).
- [138] P. Padovani, F. Oikonomou, M. Petropoulou, P. Giommi, and E. Resconi, TXS 0506+056, the first cosmic neutrino source, is not a BL Lac, *Mon. Not. Roy. Astron. Soc.* **484**, L104 (2019), [arXiv:1901.06998 \[astro-ph.HE\]](#).
- [139] A. L. Erickcek, P. J. Steinhardt, D. McCammon, and P. C. McGuire, Constraints on the Interactions between Dark Matter and Baryons from the X-ray Quantum Calorimetry Experiment, *Phys. Rev. D* **76**, 042007 (2007), [arXiv:0704.0794 \[astro-ph\]](#).
- [140] V. Gluscevic and K. K. Boddy, Constraints on Scattering of keV–TeV Dark Matter with Protons in the Early Universe, *Phys. Rev. Lett.* **121**, 081301 (2018), [arXiv:1712.07133 \[astro-ph.CO\]](#).
- [141] M. Andriamirado *et al.* (PROSPECT), Limits on sub-GeV dark matter from the PROSPECT reactor antineutrino experiment, *Phys. Rev. D* **104**, 012009 (2021), [arXiv:2104.11219 \[hep-ex\]](#).
- [142] E. Armengaud *et al.* (EDELWEISS), Searching for low-mass dark matter particles with a massive Ge bolometer operated above-ground, *Phys. Rev. D* **99**, 082003 (2019), [arXiv:1901.03588 \[astro-ph.GA\]](#).
- [143] T. Emken and C. Kouvaris, How blind are underground and surface detectors to strongly interacting Dark Matter?, *Phys. Rev. D* **97**, 115047 (2018), [arXiv:1802.04764 \[hep-ph\]](#).
- [144] E. Aprile *et al.* (XENON), First Dark Matter Search Results from the XENON1T Experiment, *Phys. Rev. Lett.* **119**, 181301 (2017), [arXiv:1705.06655 \[astro-ph.CO\]](#).
- [145] A. H. Abdelhameed *et al.* (CRESST), First results from the CRESST-III low-mass dark matter program, *Phys. Rev. D* **100**, 102002 (2019), [arXiv:1904.00498 \[astro-ph.CO\]](#).
- [146] A. H. Abdelhameed *et al.* (CRESST), Description of CRESST-III Data (2019), [arXiv:1905.07335 \[astro-ph.CO\]](#).
- [147] K. K. Rogers, C. Dvorkin, and H. V. Peiris, Limits on the Light Dark Matter–Proton Cross Section from Cosmic Large-Scale Structure, *Phys. Rev. Lett.* **128**, 171301 (2022), [arXiv:2111.10386 \[astro-ph.CO\]](#).
- [148] T. Emken, R. Essig, C. Kouvaris, and M. Sholapurkar, Direct Detection of Strongly Interacting Sub-GeV Dark Matter via Electron Recoils, *JCAP* **09**, 070, [arXiv:1905.06348 \[hep-ph\]](#).
- [149] D. Tucker-Smith and N. Weiner, Inelastic dark matter, *Phys. Rev. D* **64**, 043502 (2001), [arXiv:hep-ph/0101138](#).
- [150] E. Izaguirre, G. Krnjaic, and B. Shuve, Discovering Inelastic Thermal-Relic Dark Matter at Colliders, *Phys. Rev. D* **93**, 063523 (2016), [arXiv:1508.03050 \[hep-ph\]](#).
- [151] A. Berlin and F. Kling, Inelastic Dark Matter at the LHC Lifetime Frontier: ATLAS, CMS, LHCb, CODEX-b, FASER, and MATHUSLA, *Phys. Rev. D* **99**, 015021 (2019), [arXiv:1810.01879 \[hep-ph\]](#).
- [152] D. Merritt, M. Milosavljevic, L. Verde, and R. Jimenez, Dark matter spikes and annihilation radiation from the galactic center, *Phys. Rev. Lett.* **88**, 191301 (2002), [arXiv:astro-ph/0201376](#).
- [153] D. Merritt, Dark matter spikes and indirect detection, in *4th International Workshop on the Identification of Dark Matter* (2003) pp. 96–101, [arXiv:astro-ph/0301365](#).
- [154] G. Bertone, G. Sigl, and J. Silk, Annihilation radiation from a dark matter spike at the galactic center, *Mon. Not. Roy. Astron. Soc.* **337**, 98 (2002), [arXiv:astro-ph/0203488](#).
- [155] D. Merritt, Evolution of the dark matter distribution at the galactic center, *Phys. Rev. Lett.* **92**, 201304 (2004), [arXiv:astro-ph/0311594](#).
- [156] M. H. Chan and C. M. Lee, The first robust evidence showing a dark matter density spike around the supermassive black hole in oJ 287, *The Astrophysical Journal Letters* **962**, L40 (2024).
- [157] P. De la Torre Luque, S. Balaji, M. Fairbairn, F. Sala, and J. Silk, 511 keV Galactic Photons from a Dark Matter Spike (2024), [arXiv:2410.16379 \[astro-ph.HE\]](#).
- [158] X. Ou, A.-C. Eilers, L. Necib, and A. Frebel, The dark matter profile of the Milky Way inferred from its circular velocity curve, *Mon. Not. Roy. Astron. Soc.* **528**, 693 (2024), [arXiv:2303.12838 \[astro-ph.GA\]](#).
- [159] S. H. Lim, E. Putney, M. R. Buckley, and D. Shih, Mapping dark matter in the Milky Way using normalizing flows and Gaia DR3, *JCAP* **01**, 021, [arXiv:2305.13358 \[astro-ph.GA\]](#).